Caspofungin and LTX-315 inhibit SARS-CoV-2 replication by targeting the nsp12 polymerase

Min Wang
CAS Key Laboratory of Pathogenic Microbiology and Immunology, Institute of Microbiology, Chinese Academy of Sciences

Fei Ye
National Institute for Viral Disease Control and Prevention, Chinese Center for Disease Control and Prevention (China CDC)

Jiaqi Su
Savaid Medical School, University of Chinese Academy of Sciences

Jingru Zhao
CAS Key Laboratory of Pathogenic Microbiology and Immunology, Institute of Microbiology and Savaid Medical School, University of Chinese Academy of Sciences

Bin Yuan
CAS Key Laboratory of Pathogenic Microbiology and Immunology, Institute of Microbiology, Chinese Academy of Sciences

Baoying Huang
National Institute for Viral Disease Control and Prevention, Chinese Center for Disease Control and Prevention (China CDC)

Qi Peng
CAS Key Laboratory of Pathogenic Microbiology and Immunology, Institute of Microbiology, Chinese Academy of Sciences

Ruchao Peng
CAS Key Laboratory of Pathogenic Microbiology and Immunology, Institute of Microbiology, Chinese Academy of Sciences

Yan Sun
Savaid Medical School, University of Chinese Academy of Sciences

Suran Bai
CAS Key Laboratory of Pathogenic Microbiology and Immunology, Institute of Microbiology, Chinese Academy of Sciences

Xixi Wang
CAS Key Laboratory of Pathogenic Microbiology and Immunology, Institute of Microbiology, Chinese Academy of Sciences

Wei Yang
Savaid Medical School, University of Chinese Academy of Sciences

Zheng Fan
CAS Key Laboratory of Pathogenic Microbiology and Immunology, Institute of Microbiology, Chinese Academy of Sciences
Wenling Wang
National Institute for Viral Disease Control and Prevention, Chinese Center for Disease Control and Prevention (China CDC)
Guizhen Wu
National Institute for Viral Disease Control and Prevention, Chinese Center for Disease Control and Prevention (China CDC)
George F Gao
CAS Key Laboratory of Pathogenic Microbiology and Immunology, Institute of Microbiology, Chinese Academy of Sciences
Wenjie Tan (tanwj@ivdc.chinacdc.cn)
National Institute for Viral Disease Control and Prevention, Chinese Center for Disease Control and Prevention (China CDC)
Yi Shi (shiyi@im.ac.cn)
CAS Key Laboratory of Pathogenic Microbiology and Immunology, Institute of Microbiology; Savaid Medical School, University of Chinese Academy of Sciences; College of Basic Medicine, Jilin University, and others

---

Research Article

Keywords: SARS-CoV-2, non-structural protein 12 (nsp12) polymerase subunit2, virtual drug candidate screening, Caspofungin Acetate, LTX-315

Posted Date: March 27th, 2020

DOI: https://doi.org/10.21203/rs.3.rs-19872/v1

Abstract

The ongoing severe acute respiratory syndrome coronavirus 2 (SARS-CoV-2, previously designated as 2019-nCoV) outbreak has caused global concern1. Currently, there are no clinically approved specific drugs or vaccines available for this virus. The viral polymerase is a promising target for developing broad-spectrum antiviral drugs. Here, based on the highly similar structure of SARS- CoV non-structural protein 12 (nsp12) polymerase subunit2, we applied virtual screen for the available compounds, including both the FDA-approved and under- clinic drugs, to identify potential antiviral molecules against SARS-CoV-2. We found two drugs, the clinically approved anti-fungi drug Caspofungin Acetate (Cancidas) and the oncolytic peptide LTX-315, can bind SARS-CoV-2 nsp12 protein to block the polymerase activity *in vitro*. Further live virus assay revealed that both Caspofungin Acetate and LTX-315 can effectively inhibit SARS-CoV-2 replication in vero cells. These findings present promising drug candidates for treatment of related diseases and would also stimulate the development of pan- coronavirus antiviral agents.

Authors Min Wang, Fei Ye, Jiaqi Su, Jingru Zhao, and Bin Yuan contributed equally to this work.

Introduction

In early December 2019, a novel coronavirus SARS-CoV–2 emerged in Wuhan city in China3, and quickly spread to other regions of China and also other more than 100 countries including USA, Canada, Germany, France, Japan and South Korea1,4,5. The origins of the infection are yet to be determined. The infected patients have typical clinical symptoms such as fever, dry cough, dyspnea, headache and pneumonia6, which was designated as Corona Virus Disease 2019 (COVID–19)1. As of 27th March 2020, it has reported more than 500,000 human infections with more than 20,000 deaths. To date, no clinically approved vaccines or drugs are available for prevention and treatment of the novel coronavirus infection.

In the past years, six coronavirus species have been reported to infect humans. Among them, infections with human coronavirus–229E (HCoV–229E), HCoV-OC43, HCoV-NL63 and HCoV-HKU1 usually cause mild upper respiratory diseases similar to the common cold, while the other two highly pathogenic coronaviruses, which are responsible for severe acute respiratory syndrome (SARS) and Middle East respiratory syndrome (MERS), have caused two large-scale epidemics in the last two decades7,8. SARS-CoV–2 is the seventh human coronavirus which shows high sequence identity with the SARS-related coronaviruses found in bats9, and it uses the same cell entry receptor, angiotensin-converting Enzyme 2 (ACE2), as SARS-CoV1,10. However, the SARS-CoV–2 exhibited different pathogenesis properties compared with SARS-CoV, including higher transmission ability, and lower fatality. Therefore, it is urgent to understand the virus infection process which is important for the control and prevention of the outbreak. In addition, the emerging SARS-CoV–2 outbreak further highlights the necessity of developing broad-spectrum antiviral strategies targeting the conserved elements of the virus replication cycle.

The multi-subunit CoV RNA synthesis machinery is relatively conserved among different coronaviruses, which is responsible for the replication and transcription of the positive-sense RNA genome. The core

components of this machinery include the nsp12 RNA-dependent RNA polymerase and its cofactors nsp7 and nsp8, which is competent for nucleotide polymerization. Other additional nsps, such as nsp10, nsp13, nsp14 and nsp16, are likely necessary to carry out the full replication and transcription activities and guarantee the fidelity of RNA synthesis11–13.

The amino acid sequences of SARS-CoV–2 nsp12, nsp7 and nsp8 proteins are highly similar to their counterparts in SARS-CoV, with 96%, 97% and 99% sequence identities, respectively (Extended Data Fig. 1–2). Therefore, we can use the available structure of SARS-CoV nsp12 bound to nsp7 and nsp8 cofactors2 for virtual screening of potential drugs against the emerging SARS-CoV–2, especially within those clinically approved drugs for the emergent treatment of patients.

Results And Discussion

As shown in Fig.1, we generated a combined database with the 41,384 chemical compounds from the Target Mol, Selleck and MCE companies. After standardization operation for the chemical compounds, we obtained the 3D version of each single- molecule compound. We initially screened the compounds by the Lipinski's rule14 (rule of five) and PAINS filtration15 (to remove the compounds that might have non-specific interactions with proteins), which generated a subset of 5,762 molecules for subsequent structural docking.

We selected the conserved nsp8-binding cavity on nsp12 subunit as the target site for molecular docking using the GOLD16 software (Fig. 1a). Among the 50 top-ranking compounds in docking scores, we selected the 10 water-soluble hints as the prioritized candidates for activity assays (Extended Data Table 1).

We produced the full-length SARS-CoV–2 nsp12 protein using the baculovirus expression system, and expressed the nsp7 and nsp8 subunits in *Escherichia coli* (Chinese SARS-CoV–2 isolate BetaCov/Wuhan/WH01/2019 (EPI_ISL_406798). All these proteins were purified to high purity and homogeneity as shown by size-exclusion chromatography (SEC) and SDS-PAGE assays (Extended Data Fig. 3). Subsequently, surface plasmon resonance (SPR) experiments were performed to test the binding capacities of the 10 candidate compounds to the immobilized nsp12 protein. Among the 10 compounds, six of them showed obvious binding response, including polymyxin B sulfate (CAS number, 1405–20–5), LTX–315 (Chemical Abstracts Service (CAS) number, 1345407–05–7), Caspofungin Acetate (CAS number, 179463–17–3), Endomorphin 1 (CAS number, 189388–22–5), Fast Green FCF (CAS number, 2353–45- 9), Erioglaucine disodium salt (CAS number, 3844–45–9). Further experiments with serial-diluted concentration gradients revealed the binding affinities of the 6 candidates are 15.1 uM, 9.8 uM, 19.2 uM, 2.01 uM, 18.2 uM and 11.2 uM, respectively (Fig. 2). In addition, the binding affinities of nsp8 to nsp12 is 1.19 uM (Extended Data Fig. 4).

The *in vitro* processive RNA synthesis activity assay was performed as previously reported17, to evaluate the inhibition efficacy of the 6 nsp12-bound chemical compounds. Two of the candidate drugs, Caspofungin Acetate and LTX–315 showed good inhibition activities for RNA synthesis *in vitro (*Fig. 3).

When the molar ratio of nsp12: nsp7L8: LTX–315 or Caspofungin Acetate is 1:1:50, LTX–315 or Caspofungin Acetate can inhibit polymerase activities completely; while the molar ratio is 1:1:25, LTX–315 or Caspofungin Acetate can inhibit about half of the activities.

We further carried out standard assays to evaluate the cytotoxicity of the two enzymatically inhibitory compounds and to test the inhibition efficacy for SARS-CoV-2 replication at cell level. The cytotoxicity of the compounds in vero cells (ATCC, CCL-81) was determined by the CCK–8 assay. Then, vero cells were infected with BetaCov/Wuhan/WH01/2019 in the presence of drugs with varying concentrations. Efficacies were evaluated by quantifying the virus copy numbers in the cell supernatant via quantitative real-time RT-PCR (qRT-PCR). LTX–315 (half-maximal effective concentration (EC50) = 32.17 μM, the half cytotoxic concentration (CC50) > 50 μM) can inhibit the virus replication in cells but has strong cytotoxicity under the 100 μM concentration that show nearly 100% inhibition activity (Fig. 4). Notably, Caspofungin Acetate (EC50 = 19.41 μM, CC50 > 100 μM) can effectively inhibit virus replication in cells (Fig. 4) without obvious cytotoxicity.

LTX–315 is currently tested in phase I/II clinical trials, as a potential first-in-class oncolytic 9-mer peptide18. Therefore, LTX–315 can result in cytotoxicity in vero cells under high concentrations, as vero cells are transformed cells that have some characteristics of cancer cells. LTX–315 is a derivative of the host defense peptide (HDP) bovine lactoferricin19. HDPs have been found in a wide variety of species as part of the host defense system against pathogens and are rich in basic and hydrophobic amino acid residues20. It has been revealed that the biological activity of the HDPs often relies on the peptide-membrane interactions in addition to possible intracellular targets21. The instability of LTX–315 in human plasma results from the sequential exopeptidase- mediated cleavage at the N-terminus, and the half-life of LTX–315 was determined to be 160 minutes20. The animal protection experiment should be conducted in the future to test the *in vivo* efficacy of LTX–315. Molecular docking of LTX–315 on nsp12 structure shows that the peptide fills the nsp8 binding cavity and the C-terminal portion forms intensive interactions with the open edge of the cavity (Extended Data Fig. 5). The information of LTX–315 provides a promising starting point for designing anti- coronavirus drugs, and also gives a drug choice of compassionate use for the infected cancer patients.

Caspofungin has been approved to treat the candidal esophagitis and deep-seated candidal infections, and is also an alternative therapy for *Aspergillus* infections22. The inhibition mechanism of Caspofungin is to non-competitively inhibit the synthesis of 1,3-β-glucans which are key components of fungal cell walls23. The enzymatic system for 1,3-β-glucan synthesis is absent in mammalian cells22. Caspofungin is a cyclic- hexapeptide compound with a fatty acid side chain and is available in an intravenous formulation but lacks an oral formulation24. Molecular docking of Caspofungin in the nsp8 binding cavity on nsp12 structure shows that the cyclic-hexapeptide moiety is accommodated within the cavity and the fatty acid side chain reaches out to interact with the edge region (Extended Data Fig. 5).

Recent clinical studies have revealed that severe SARS-CoV–2 infected patients probably have fungal coinfection during the disease progression25. Thus, the discovery of Caspofungin against SARS-CoV–2

infection can provide a nice choice for the dual- function treatment of the patients, inhibiting both SARS-CoV–2 and fungi infections. Since Caspofungin has been used in human patients with a safety track record, we suggest that it should be evaluated in patients suffering from the COVID–19.

References

1. <https://who.int/emergencies/diseases/novel-coronavirus-2019/events- as-they-happen>
2. Kirchdoerfer, R. N. & Ward, B. Structure of the SARS-CoV nsp12 polymerase bound to nsp7 and nsp8 co-factors. *Nat Commun* **10**, 2342, doi:10.1038/s41467-019-10280-3 (2019).
3. Zhu, N. *et al.* A Novel Coronavirus from Patients with Pneumonia in China, 2019. *N Engl J Med* **382**, 727-733, doi:10.1056/NEJMoa2001017 (2020).
4. Holshue, L. *et al.* First Case of 2019 Novel Coronavirus in the United States. *N Engl J Med*, doi:10.1056/NEJMoa2001191 (2020).
5. Kim, Y. *et al.* The First Case of 2019 Novel Coronavirus Pneumonia Imported into Korea from Wuhan, China: Implication for Infection Prevention and Control Measures. *J Korean Med Sci* **35**, e61, doi:10.3346/jkms.2020.35.e61 (2020).
6. Huang, C. *et al.* Clinical features of patients infected with 2019 novel coronavirus in Wuhan, China. *Lancet* **395**, 497-506, doi:10.1016/S0140- 6736(20)30183-5 (2020).
7. Zhong, N. S. *et al.* Epidemiology and cause of severe acute respiratory syndrome (SARS) in Guangdong, People's Republic of China, in February, 2003. *Lancet* **362**, 1353-1358, doi:10.1016/s0140-6736(03)14630-2 (2003).
8. Zaki, M., van Boheemen, S., Bestebroer, T. M., Osterhaus, A. D. & Fouchier, A. Isolation of a novel coronavirus from a man with pneumonia in Saudi Arabia. *N Engl J Med* **367**, 1814-1820, doi:10.1056/NEJMoa1211721 (2012).
9. Lu, R. *et al.* Genomic characterisation and epidemiology of 2019 novel coronavirus: implications for virus origins and receptor binding. *Lancet* **395**, 565-574, doi:10.1016/S0140-6736(20)30251-8 (2020).
10. Zhou, *et al.* A pneumonia outbreak associated with a new coronavirus of probable bat origin. *Nature*, doi:10.1038/s41586-020-2012-7 (2020).
11. Ma, *et al.* Structural basis and functional analysis of the SARS coronavirus nsp14-nsp10 complex. *Proc Natl Acad Sci U S A* **112**, 9436-9441, doi:10.1073/pnas.1508686112 (2015).
12. Decroly, *et al.* Crystal structure and functional analysis of the SARS- coronavirus RNA cap 2'-O-methyltransferase nsp10/nsp16 complex. *PLoS Pathog* **7**, e1002059, doi:10.1371/journal.ppat.1002059 (2011).
13. Su, D. *et al.* Dodecamer structure of severe acute respiratory syndrome coronavirus nonstructural protein nsp10. *J Virol* **80**, 7902-7908, doi:10.1128/JVI.00483-06 (2006).
14. Lipinski, C. A., Lombardo, , Dominy, B. W. & Feeney, P. J. Experimental and computational approaches to estimate solubility and permeability in drug discovery and development settings. *Adv Drug Deliv*

Rev **46**, 3-26, doi:10.1016/s0169-409x(00)00129-0 (2001).

15. Baell, J. B. & Holloway, G. A. New Substructure Filters for Removal of Pan Assay Interference Compounds (PAINS) from Screening Libraries and for Their Exclusion in Bioassays. *J Med Chem* **53**, 2719-2740 (2010).
16. Jones, G., Willett, , Glen, R. C., Leach, A. R. & Taylor, R. Development and validation of a genetic algorithm for flexible docking. *J Mol Biol* **267**, 727-748, doi:10.1006/jmbi.1996.0897 (1997).
17. Subissi, L. *et al.* One severe acute respiratory syndrome coronavirus protein complex integrates processive RNA polymerase and exonuclease activities. *Proc Natl Acad Sci U S A* **111**, E3900-3909, doi:10.1073/pnas.1323705111 (2014).
18. Sveinbjornsson, , Camilio, K. A., Haug, B. E. & Rekdal, O. LTX-315: a first- in-class oncolytic peptide that reprograms the tumor microenvironment. *Future Med Chem* **9**, 1339-1344, doi:10.4155/fmc-2017-0088 (2017).
19. Tomita, *et al.* Potent antibacterial peptides generated by pepsin digestion of bovine lactoferrin. *J Dairy Sci* **74**, 4137-4142, doi:10.3168/jds.S0022- 0302(91)78608-6 (1991).
20. Haug, B. E. *et al.* Discovery of a 9-mer Cationic Peptide (LTX-315) as a Potential First in Class Oncolytic Peptide. *J Med Chem* **59**, 2918-2927, doi:10.1021/acs.jmedchem.5b02025 (2016).
21. Brogden, K. A. Antimicrobial peptides: pore formers or metabolic inhibitors in bacteria? *Nat Rev Microbiol* **3**, 238-250, doi:10.1038/nrmicro1098 (2005).
22. Morrison, A. Caspofungin: an overview. *Expert Rev Anti Infect Ther* **3**, 697- 705, doi:10.1586/14787210.3.5.697 (2005).
23. Douglas, M. Understanding the microbiology of the Aspergillus cell wall and the efficacy of caspofungin. *Med Mycol* **44**, S95-S99, doi:10.1080/13693780600981684 (2006).
24. Jokela, J. A. & Kaur, Caspofungin-resistant oral and esophageal candidiasis in a patient with AIDS. *AIDS* **21**, 118-119, doi:10.1097/QAD.0b013e3280117f5f (2007).
25. Yang, *et al.* Clinical course and outcomes of critically ill patients with SARS- CoV-2 pneumonia in Wuhan, China: a single-centered, retrospective, observational study. *Lancet Respir Med*, doi:10.1016/S2213-2600(20)30079-5 (2020).
26. Robert, X. & Gouet, Deciphering key features in protein structures with the new ENDscript server. *Nucleic Acids Res* **42**, W320-324, doi:10.1093/nar/gku316 (2014).

Methods

Virtual screen of the chemical compounds

For molecular docking, the 3.1 Å cryo-EM structure of SARS-CoV nsp12 subunit in its complex with nsp7 and nsp8 (PDB ID: 6NUR) was extracted as the receptor. The starting compound library was collected from TargetMol, MedChemExpress and Selleckchem companies, which was initially cleaned by the Lipinski's rule of five (Structures violating more than three of Lipinski's rules were discarded)14 and Pan

Assay Interference Compounds (PAINS) structure 15. The remaining compounds were docked into the nsp8-binding site of nsp12 using GOLD16 program. The parameter files for docking was prepared using Hermes (ref.). The box dimension for docking calculation was set to 10 Å (centered at residue P116) to allow enough space for orientation sampling.

Protein expression and purification

The genes for full-length nsp7 and nsp8 of SARS-CoV–2 isolate BetaCov/Wuhan/WH01/2019 (EPI_ISL_406798) were synthesized by Synbio Technologies, which were codon-optimized for *Escherichia coli E. coli)* and cloned into pET–21a plasmid for protein expression. The nsp8 subunit was fused with an N- terminal 6 × His-tag to facilitate purification. The nsp7L8 fusion construct was generated by introducing a 6×His-linker between nsp7 and nsp8 coding sequences. Both the nsp8 subunit and nsp7L8 fusion protein were expressed in *E. coli* BL21 (DE3).

The transformed bacteria were cultivated at 37 °C to an OD600 nm of 0.6 and then supplemented with 1 mM isopropyl β-D–1-thiogalactopyranoside to induce protein expression at 16 °C for an additional 14–18 h. Cells were harvested by centrifugation and resuspended in a buffer containing 20 mM HEPES pH 7.5, 500 mM NaCl, 2 mM Tris(2-carboxyethyl)phosphine (TCEP), which were homogenized at 4 °C with a ultrahigh-pressure cell disrupter (JNBIO, China). The lysate was cleared by centrifugation at 12,000× rpm for 60 min and passed through 0.22-μm filter films (Millipore). Recombinant proteins were captured by Ni-NTA affinity chromatography using a HisTrapHP column (GE Life Sciences), and further purified by size-exclusion chromatography (SEC) using a Superdex 200 increase 10/300 column (GE Life Sciences). The eluted fractions were analyzed by SDS-PAGE and concentrated with an Amicon Ultra concentrator (Millipore).

The gene for SARS-CoV–2 nsp12 was chemically synthesized with codon optimization for insect cells (*Spodoptera frugiperda)* by Synbio Technologies. The sequence was fused with a C-terminal thrombin cleavage site, a 6×His-tag and a 2×Strep-tag (LVPRGSHHHHHHGWSHPQFEKGGGSGGGSGGSAWSHPQFEKGS), and incorporated into pFastbac–1 plasmid. Recombinant protein was expressed with High Five cells at 27 °C for 48 h post infection. Cells were harvested by centrifugation at 2,000× rpm for 30 min, and resuspended in a buffer consisting of 25 mM HEPES pH 7.4, 1 M NaCl, 1 mM MgCl2 and 2mM TCEP. An equal volume of the same buffer supplementaed with 0.2% (v/v) Igepal CA–630 (Anatrace) was added and incubated at 4 ° C for 10 min. Cells were lysed by sonication and the lysate was clarified by ultracentrifugation at 30,000× rpm for 2 h. Cleared lysates were passed through a 0.22-μm filter film before further purification. The protein was purified by tandem affinity chromatography using a StrepTrapHP (GE Life Sciences) and SEC using a Superdex 200 increase 10/300 column (GE Life Sciences). The SEC buffer consists of 25 mM HEPES pH 7.5, 300 mM NaCl, 0.1 mM MgCl2 and 2 mM TCEP. The eluted fractions were analyzed by SDS-PAGE and concentrated with an Amicon Ultra concentrator (Millipore).

Drugs

Caspofungin Acetate (Cat no. T1799), Polymyxin B sulfate (Cat no. T1100), LTX–315 (Cat no. T6881), Fast Green FCF (Cat no. T7772), Erioglaucine disodium salt (Cat no. T7771) were obtained from TargetMol. TB500 (Cat no. HY-P0170), Degarelix (Cat no. HY–16168A), Endomorphin 1 (Cat no. HY-P0185), Lysipressin (Cat no. HY-P0004), A 779 (Cat no. HY-P0216) were obtained from MedchemExpress. All drugs were dissolved in distilled water to prepare 10 mM stock solutions, and stored at –20℃.

Cells

Vero cell line (ATCC, CCL–81) was cultured at 37 °C in Dulbecco's modified Eagle's medium (DMEM, Gibco, Grand Island, USA) supplemented with 10% fetal bovine serum (FBS, Gibco) in the atmosphere with 5% CO2. Cells were digested with 0.25% trypsin and uniformly seeded in 96-well plates with a density of 1×104 cells/well prior infection or drug feeding.

Cell viability analysis

Vero cells were treated with drugs at different concentrations for 24 h or 48 h in 5% CO2 at 37 °C. Cell viability was tested by CCK–8 (MedchemExpress, Monmouth Junction, USA) assay. Briefly,10 μl of CCK–8 was added to the medium and incubated with cells for 1–4 h. Absorbance value was measured at 450 nm wavelength using a microplate reader (Thermo Fisher Scientific, Waltham, USA).

Surface plasmon resonance (SPR) assay

The affinities between nsp12 and nsp8 or drugs were measured at room temperature (r.t.) using a Biacore 8K system with CM5 chips (GE Healthcare). The nsp12 protein was immobilized on the chip with a concentration of 100 μg/mL (diluted by 0.1mM NaAc, PH 4.0).

For nsp8 measurements, a solution containing 25 mM HEPES pH 7.5, 300 mM NaCl, 0.1 mM MgCl2, 2 mM TCEP and 0.005% tween–20 was used as running buffer. The nsp8 protein was pre-exchanged into the running buffer by SEC prior loading to the system. A blank channel of the chip was used as the negative control. Serial diluted nsp8 solution was then flowed through the chip surface. The single-cycle binding kinetics was analyzed with the Biacore 8K Evaluation Software (version1.1.1.7442) and fitted with a 1:1 binding model.

For the measurement of drugs, 1×PBST (phosphate buffer saline supplemented with 0.005% tween–20) was used for running and diluting drugs. Each drug with gradient concentrations was flowed through the chip surface. The multi-cycle binding kinetics were analyzed with a Biacore 8K system, which were fitted using a steady state binding model.

In vitro polymerase inhibition assay

A 40-nt template RNA (LS1) corresponding to the 3' end of the SARS-CoV–2 genome and a complementary 20-nt primer (LS2) containing a 5' fluorescein label were chemically synthesized by Logen Biotech LLC. LS1 was annealed to LS2 by heating at 70 °C for 10 min and then cooling down to 4 °C. The inhibition of drugs to SARS- CoV–2 nsp12 polymerase was tested using a modified primer extension assay. The reaction systems contained 1 μM nsp12, 1 μM nsp7L8, 1 μM annealed primer/template, ~50 μM drugs dissolved in a reaction buffer containing 10 mM Tris-HCl, pH 8.0, 10 mM KCl, 2 mM MgCl2 and 1 mM beta-mercaptoethanol. Reactions were initiated by adding 500 μM GTP, 500 μM UTP, 500 μM CTP and 500 μM ATP, which were incubated at 30 °C for 60 min and stopped by mixing with equal-volume formamide loading buffer (Coolaber). The RNA products were resolved by denaturing TBE-Urea PAGE and visualized with a Fusion fx (Vilber Lourmat) imaging system.

Inhibition of virus replication in vero cells

Vero cells were infected with SARS-CoV–2 (nCoV- BetaCov/Wuhan/WH01/2019) with a dose of 100 TCID50/well. After 2 h incubation at 37°C in 5% CO2 atmosphere, the supernatant was discarded and plates were washed with 1×PBS. An aliquot of 200 μL serial-diluted drugs were added into the plate and incubated at 37 °C for an additional 24 h or 48 h. The efficacies of drugs were evaluated by quantifying virus copy numbers in the supernatant via quantitative real-time RT-PCR (qRT-PCR).

Statistical analysis

Quantitative analysis of polymerase inhibition experiment was performed by Image J. The Virus suppression curves and histograms were plotted by Graphpad prism 6 software. EC50 and CC50 values were calculated by SPSS. Data were represented as mean ± standard error of mean. Statistical significance between two groups was determined using two-tailed Student’s t-test. p values < 0.05 were considered significant.

Declarations

Data availability

All data presented in this manuscript are shown in the main text figures and Extended Data. All other materials and resources are available from the authors on reasonable request.

Acknowledgements

We thank staffs of Core Facility in Institute of Microbiology, CAS, for assistance in SPR experiments. This study was supported by the National Science and Technology Major Project (2018ZX10101004), the

Strategic Priority Research Program of CAS (XDB29010000) and National Natural Science Foundation of China (NSFC) (82041016 and 81871658). M. W. is supported by the National Science and Technology Major Project (2018ZX09711003) and National Natural Science Foundation of China (NSFC) (81802007). R. P. is supported by the Young Elite Scientist Sponsorship Program (YESS) by China Association for Science and Technology (CAST) (2018QNRC001). Y. S. is also supported by the Excellent Young Scientist Program and from the NSFC (81622031) and the Youth Innovation Promotion Association of CAS (2015078).

Author contributions

Y. S. and W. T. conceived the study. J. S. conducted molecular docking, M. W., J. Z., B. Y., X. W. and Q. P. purified the protein samples and conducted biochemical studies. F. Y., S. B., B. H. conducted cell-based assays. M. W., R. P., F. Y., Y.Sun, S. B., J. Z., B. H., W. Y., Q. P., W. T. and Y. S., analyzed the data. M. W., R. P., J. Z., J. S., Y.Sun, and Y. S. wrote the manuscript. All authors participated in the discussion and manuscript editing. M. W., F. Y., J. S., J. Z. and B. Y. contributed equally to this work.

Competing interests

The authors declare no competing interests.

Figures

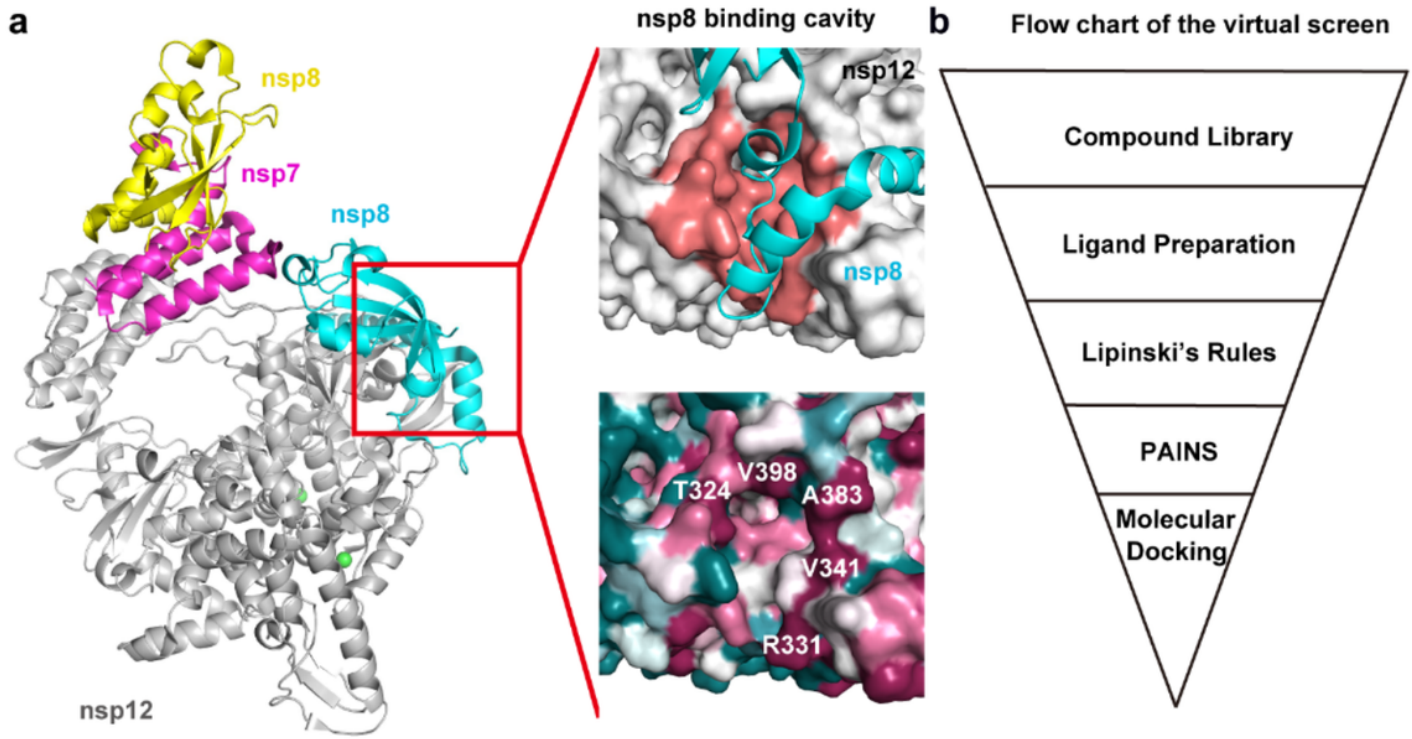

Figure 1

The conserved nsp8-binding cavity on SARS-CoV nsp12 polymerase. a, Structure of SARS-CoV nsp12 bound to nsp7 and nsp8 co-factors (PDB ID: 6NUR). The upper inset displays the nsp8-binding cavity (colored in salmon) on nsp12 polymerase, which was used for Molecular docking. The lower panel inset displays the degree of conservation of the pocket calculated by aligning all seven HCoV homologues sequences, with the most conserved region colored in dark magenta and the most variable region in dark cyan. b, Flow chart of virtual screen.

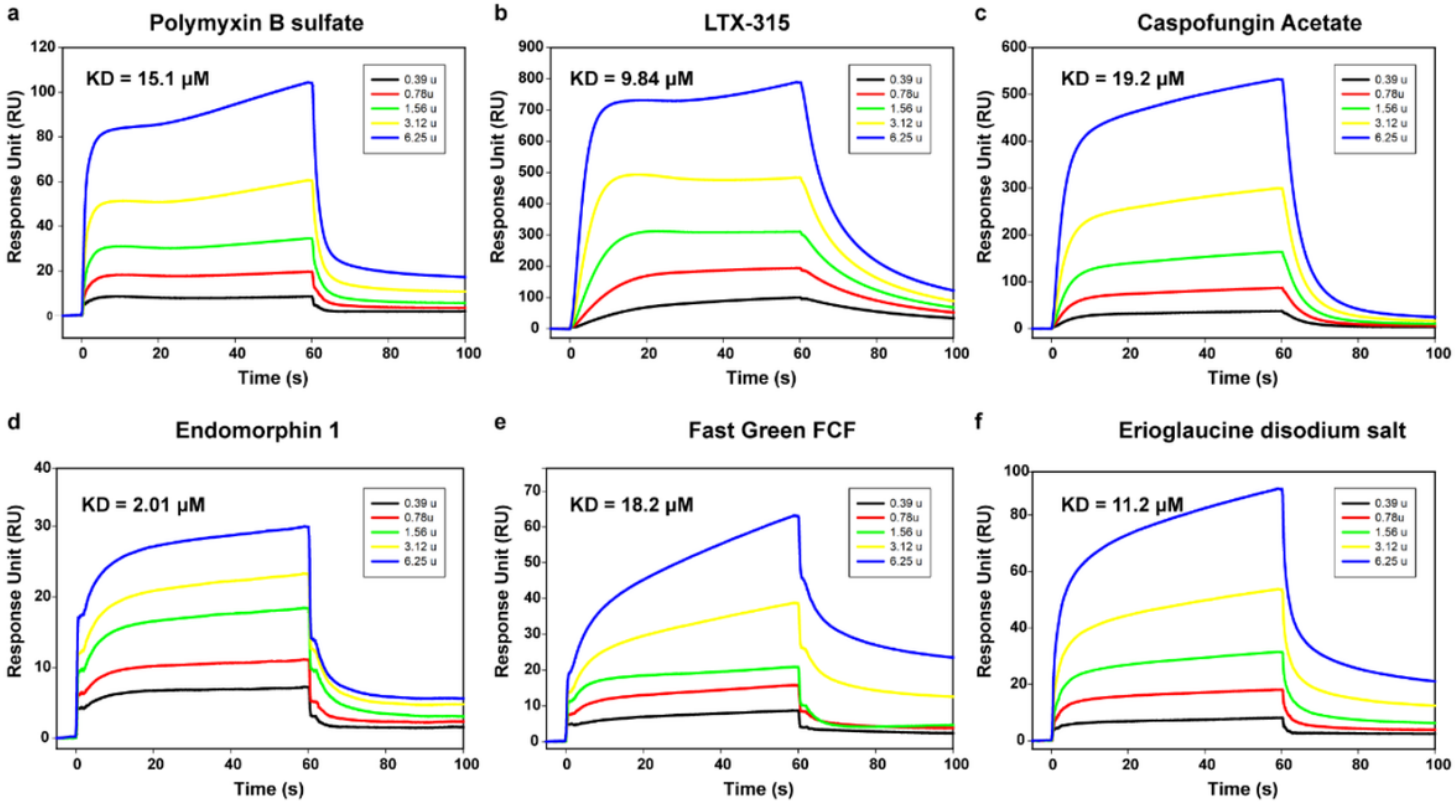

Figure 2

Biophysical interaction profiles of the 6 candidate compounds to SARS- CoV-2 nsp12 polymerase protein. SARS-CoV-2 nsp12 polymerase protein was immobilized on the chip and tested for binding with gradient concentrations of candidate compounds. The binding profiles of different drugs are shown in individual panels. Polymyxin B sulfate (a); LTX-315 (b); Caspofungin Acetate (c); Endomorphin 1 (d); Fast Green FCF (e); Erioglaucine disodium salt (f). The raw binding curves are shown in the figure. The data shown is a representative result of two independent experiments using different protein preparations.

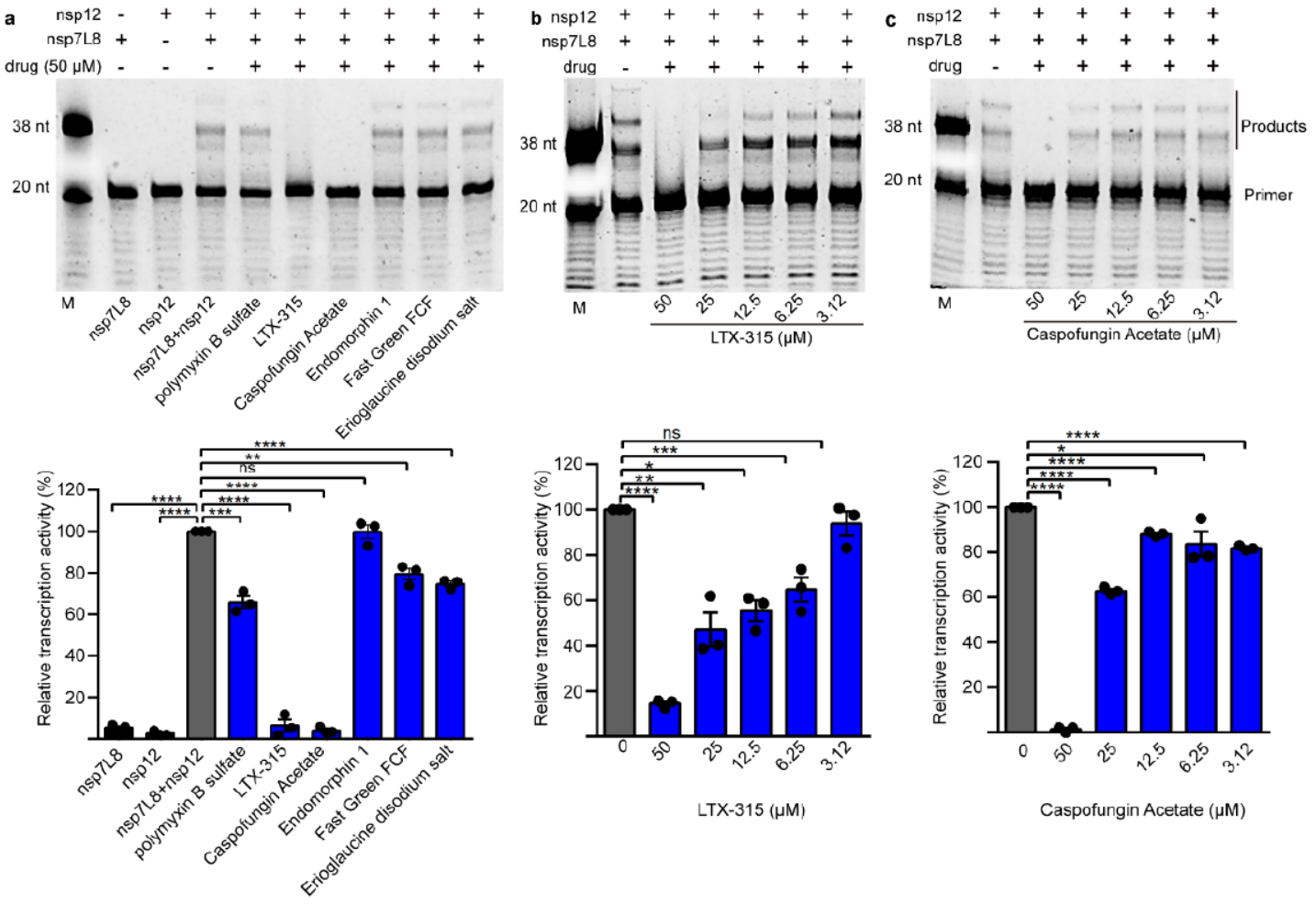

Figure 3

Inhibition of the 6 nsp12-bound candidate compounds to nsp12 polymerase activity in vitro. Polymerase activity assay was conducted using nsp12 and cofactors nsp7 and nsp8, in the presence or absence of candidate compounds (50 μM). Two main products were observed through primer extension experiments without compounds. The six nsp12-bound candidate compounds (50μM) showed different inhibitory activities (a). Dose-dependent inhibition of LTX-315 (b) and Caspofungin Acetate (c) for SARS-CoV-2 polymerase activities. The data shown is a representative result of three independent experiments using different protein preparations. The relative quantities of each product were quantified by integrating the intensities of the bands on ImageJ. Inhibition rate was analyzed using GraphPad software. All data are presented as mean ± SEM. n= 3, * $p < 0.05$; ** $p < 0.01$; *** $p < 0.001$; **** $p < 0.0001$. ns, not significant.

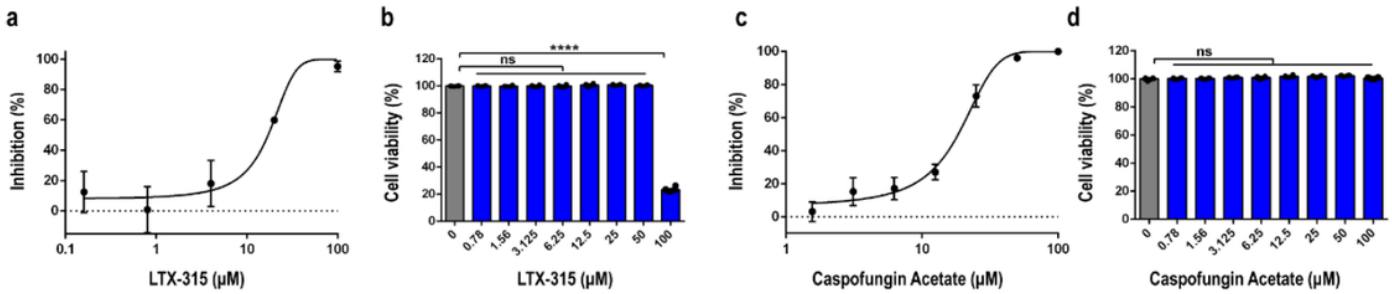

Figure 4

The antiviral activities of Caspofungin Acetate and LTX-315 against SARS- CoV-2 infection in vero cells. Vero cells were infected with SARS-CoV-2 with 100 TCID50/well, and drugs in different concentrations were administered at 2 hpi. After an additional 24 h (LTX-315) or 48 h (Caspofungin Acetate) incubation, viral titer in the cell supernatant were quantified by qRT-PCR (a and c). Viability of vero cells treated by drugs was measured by CCK-8 assays (b and d). The data shown are representative results of three independent experiments using different sample preparations. All data are presented as mean ± SEM. n = 6, **** $p < 0.0001$. ns, not significant.

Supplementary Files

This is a list of supplementary files associated with this preprint. Click to download.

- Extendeddata.pdf